Contents list available at IJRED website

International Journal of Renewable Energy Development

Journal homepage: https://ijred.undip.ac.id

Research Article

# Effect of natural dye combination and pH extraction on the performance of dye-sensitized photovoltaics solar cell

Indri Wasa Estiningtyas[a], Nita Kusumawati[a*], Pirim Setiarso[a], Supari Muslim[b], Nunik Tri Rahayu[a], Riska Nur Safitri[a], Nafisatus Zakiyah[a], Fadlurachman Faizal Fachrirakarsie[a]

[a]*Department of Chemistry, Faculty of Mathematics and Natural Science, Universitas Negeri Surabaya, Surabaya, 60231, Indonesia*

[b]*Department of Electrical Engineering, Faculty of Engineering, Universitas Negeri Surabaya, Surabaya, 60231, Indonesia*

**Abstract**. Dyes are significant components in Dye Sensitized Solar Cell (DSSC) performance because they act as photosensitizers. Natural dye-based DSSC system fabrication innovations continue to be produced in an effort to improve DSSC performance efficiency. In this study, a DSSC system was developed using double components of natural dyes as natural photosensitizers to enhance DSSC efficiency. This method of making natural dye-based DSSC uses a combination of dye extracts from two different dye sources that have the potential as natural photosensitizers in DSSC. The research aims to investigate the impact of the combined use of two natural dyes and pH variations on DSSC performance. DSSC performance measurements encompass the short-circuit current (Isc), open-circuit voltage (Voc), and DSSC efficiency parameters. The obtained results indicate efficiency values for dyes (a) sappan wood/ethanol and turmeric/methanol; (b) turmeric/methanol and beetroot/ethanol; and (c) beetroot/ethanol and turmeric/distilled water. At neutral pH, the efficiency values are 2.09%, 2.10%, and 2.19%, respectively. Meanwhile, at acidic pH of 2.59%; 2.39%; and 2.71%. Notably, the dye efficiency values at acidic pH surpass those found at neutral pH conditions. The highest efficiency is observed in the combination of dye (c) beetroot/ethanol and turmeric/distilled water with efficiency reaching 2.71% at acidic pH.

**Keywords:** Dye Sensitized Solar Cell, Natural dyes, Photosensitizer, Short-Circuit Current, Open-Circuit Voltage, Efficiency.



Received: 5th July 2023; Revised: 26th Sept 2023 Accepted: 3rd Oct 2023; Available online: 16th Oct 2023

## 1. Introduction

Energy is an essential component of all human activities (Hdom & Fuinhas, 2020). Humans will have challenges if energy is limited (Ganiyu *et al.,* 2020). Accordingly, the majority of energy used today, namely non-renewable fossil energy, is depleting petroleum resources, so it is necessary to use alternative energy sources (Wu *et al.*, 2021). Renewable energy is an alternative way to prevent fossil scarcity in the future (Panagopoulos, 2021). One of the abundant renewable energy sources is solar energy, with an estimated capacity of 150.73 PWh in 2050 (Ji *et al.*, 2022). Consequently, to generate electricity, solar panel systems are required (Alirahmi *et al.*, 2020). Dye-sensitized solar cells (DSSC) are solar cells that transform solar energy into electrical energy by using semiconductor materials (Moharam *et al.*, 2021). Solar cells have attracted many researchers due to their high efficiency, environmental friendliness, and ease of manufacture (Kusumawati *et al.*, 2018; Noorasid *et al.,* 2022). The components of DSSC's are working electrode (WE), dye or sensitizer, an electrolyte, and the counter electrode (CE) (Sunder, *et al.*, 2021)

Electrolytes are a key component of DSSC (Selvanathan *et al.*, 2020). In general, the type of electrolyte used in DSSCs is liquid electrolyte. Liquid electrolytes outperform gels and solid electrolytes (Bandara *et al.,* 2018). However, the issue of liquid electrolyte leakage frequently arises, posing potential obstacles. Furthermore, the limited longevity of liquid electrolytes has implications for the enduring performance and stability of DSSC (Önen *et al.*, 2019). To overcome these problems, polymer-based electrolytes that have high ionic conductivity, tensile strength, flexibility, no leakage and long-term performance are made (Bußmann *et al.*, 2021; Morsada *et al.*, 2021). Polyvinylidene fluoride (PVDF) membrane can therefore be employed as a polymer material to conceal the weak point of the liquid electrolyte in the event of seal leakage (Pradhan & Chakraborty, 2020).

The performance of DSSCs is significantly influenced by the role played by dye sensitizers (Ganta et al., 2019). Different varieties of dyes, including both organic and inorganic types, were employed in DSSCs (Rekha *et al.,* 2019; Sharma *et al.,* 2018). Currently, inorganic dyes such as Ruthenium are acknowledged as the most significant dyes for manufacturing DSSCs due to their remarkable efficiency (Jalali *et al.,* 2020). However, these types of dyes tend to be costly, possess toxic properties, and present challenges in terms of their purification (Rekha *et al.,* 2019). Recently, there has been extensive research into natural dyes because of their significant absorption in the visible spectrum, widespread availability in nature,

* Corresponding author:
Email: nitakusumawati@unesa.ac.id (N. Kusumawati)

https://doi.org/10.14710/ijred.2023.56172
ISSN: 2252-4940/© 2023.The Author(s). Published by CBIORE

straightforward sample preparation, cost-effectiveness, and eco-friendliness (Jalali *et al.,* 2020).

According to another study, pH modulation of dyes as sensitizers can be utilized as an alternate approach to disguise dye stability (Golshan *et al.*, 2021). In the research of Mejica, et al (2022), optimisation of malabar spinach *(Basella alba*) as a single sensitizer with pH variation was obtained, the best light to electricity conversion efficiency was observed at pH 9, with an efficiency of 0.1021%, electric current of 0.0682 mA, voltage of 0.4877 V, and power density of 0.0227 mW/cm$^2$. (Mejica *et al.,* 2022). Research by Golshan et al, 2021, has investigated the effect of co-sensitization in dye-sensitized solar cells using dye extracts from *Malva verticillate* and *Syzygium cumini* as a single sensitized. The solar cell obtained has an efficiency of 0.05% for *Malva verticillate* and 0.03% for *Syzygium cumini* at neutral pH. On the other hand, the dye cocktail of *Malva verticillate* and *Syzygium cumini* gave an efficiency of 0.05% in alkaline medium and 0.6% in acidic medium. The better performance in acidic medium is due to the reduced steric hindrance and multiple anchor groups to the $TiO_2$ surface (Golshan *et al.*, 2021). Junger *et al.* (2019) stated that the efficiency of dye-based DSSC depends on the pH content of the solution due to hyperchromic or hypochromic effects. It was reported that the efficiency of the dye cell increased from neutral pH to acidic pH by 50%. Dye cells at pH 1 have the highest efficiency, namely 0.058% (Junger *et al.* 2019). According to research by Rajaraman, et al (2022), two dyes combined enhance light absorption thereby increasing the efficiency and stability of DSSCs (Rajaraman *et al.,* 2022).

This research aims to determine the effect of the combination of two natural dyes which are sappan wood/ethanol and turmeric/methanol, turmeric/methanol and beetroot/ethanol, beetroot/ethanol and turmeric/distilled water at acidic pH and neutral pH using polyvinylidene fluoride (PVDF) polymer electrolyte on the performance of dye-sensitized solar cells. The use of a combination of natural materials to enhance DSSC performance and this approach is considered an alternative to employing inorganic dyes, particularly when comparing performance at both acidic and neutral pH conditions.

## 2. Materials and Methods

### *2.1 Materials*

Polyvinylidene fluoride (PVDF) (powder, Mw~534,000), Titanium dioxide ($TiO_2$) (21 nmF nanopowder; 99.5%), Ethylene carbonate (EC) (99% anhydrous), Propylene carbonate (PC) (99.7% anhydrous), Polyethylene glycol ($C_{2n}H_{4n+2}O_{n+1}$) (Mw 1000), Nitric acid ($HNO_3$) (≥99.9%)., Hydrochloric Acid (HCl) and Aceton ($CH_3COCH_3$) (≥99.5%) were purchased from Sigma Aldrich, USA; Tween-80 (PT. Brataco Chemika; Indonesia); Ethanol ($C_2H_6O$), Methanol ($CH_3OH$), and Iodine ($I_2$) (≥99.8%); were purchased from PT. Smart Lab, Indonesia. Potassium iodide (KI), Sodium Hydroxide (NaOH), N, N-Dimethylacetamide (DMAc) were purchased (≥ 99%) from Merck Germany, and Changchun Yutai Optics Co., Ltd. (China) provided fluorine-doped tin oxide (FTO) (resistivity 10) glass. All reagents are of analytical grade. Sappan wood, turmeric, and beetroot were procured from the local market

### *2.2 Methods*

#### *2.2.1 Double Colour Component Blend Manufacture*

The dye source components were extracted by maceration using various solvents such as distilled water, methanol, and ethanol in a ratio of 1:6 with a variation of 0.5–24 hours. The product extracted from the two different dyes was filtered using filter paper Whatman no 1, then the filtrate of the two dyes was homogenized, after which the 80 mL dye solution was evaporated for 4 minutes. The evaporated dye was then conditioned at the original pH 7 solution (without pH conditioning) and acidic pH. 0.1 M HCl was used to condition the acidity of the solution to reach pH 4.

#### *2.2.2 Making of $TiO_2$ paste*

$TiO_2$ paste prepared by mixing 0.2 g titanium oxide ($TiO_2$), 0.08 g propylene glycol (PEG-1000), 0.4 mL 0.1 M nitric acid ($HNO_3$) solution, and 0.05 mL tween-80, all while stirred for 30 minutes at 100 rpm.

#### *2.2.3 Making polymer-electrolyte Membrane*

A polymer-electrolyte membrane is formed in two steps: initially, an electrolyte solution is prepared, followed by the creation of a PVDF membrane. The magnetic stirrer (NESCO LAB MS-H280-Pro magnet) was employed for 30 minutes to blend 9.2 mg of solid iodine ($I_2$), 0.06 g of potassium iodide, 0.4 g of propylene carbonate (PC), and 0.4 g of ethylene carbonate (EC). PVDF membranes are manufactured utilizing phase separation, electrospinning, and casting knife techniques (Kusumawati *et al.,* 2018). PVDF was dissolved in a 3:2 mixture of DMAc and acetone on a hot plate magnetic stirrer at 65°C and 270 rpm for 12 hours to get an 18% (w/v) PVDF solution (Kusumawati, *et al.,* 2018).

Membrane with casting knife technique, An 18% (w/v) PVDF solution was cast on glass with thickness variations of 0.6 mm, 0.4 mm, and 0.2 mm at 30 °C with an initial immersion period of 5 minutes, then immersed in 1000 mL of water distillate non-solvent coagulation bath for 30 minutes at 30 °C.. The solid PVDF membrane was then washed twice in 500 mL of non-solvent distilled water for 1 minute each time before resting for 24 hours at 25 °C room temperature. Membrane electrospinning casting technique, 18% (w/v) PVDF solution, 5 cm, 10 cm, and 15 cm distances between injection and drum collector, a flow rate of 1 mL/hour, and a voltage of 15 kV for 5 hours were used.

#### *2.2.4 Fabrication of DSSC*

Two FTO glasses, an FTO anode, and a cathode comprise the DSSC system circuit. Semiconductor $TiO_2$ was sintered for 1 hour at 450 °C after being coated on FTO glass with an active area of 3 cm$^2$ using the doctor blade method. For duration of 24 hours, the sintered product was immersed in 10 mL of dye extract. Subsequently, a PVDF-NF membrane measuring 2x1.5 cm was soaked in 1 mL of electrolyte for 1 hour before being positioned on a carbon-coated FTO cathode.

#### *2.2.5 Characterization of DSSC*

The UV-Vis spectrum of the pigment was analyzed using the Shimadzu UV-1800 UV-Vis spectrophotometer. Current and potential changes were analyzed using Voltammetry 797 VA Computrace by Metrohm. The current measurement of the circuit were conducted using a Krisbow KW08-267 Multimeter.

#### *2.2.6 Measurement of the photoelectric parameters of DSSC*

Under the simulated white light source (100 mW/cm$^2$ and AM 1.5), the current-voltage (I-V) curve was observed. The energy conversion efficiency can be defined as follows:

$$\eta = \frac{Isc \times Voc \times FF}{P_{in}} \quad (1)$$

Where, Fill factor (FF) = = $\frac{V_{max} \times I_{max}}{Voc \times Isc}$ , $V_{max}$= maximum output voltage, $I_{max}$= maximum output current, Voc = Open circuit voltage, Isc = Short-circuit currentand Pin = Incident photon energy.

## 3. Result and Discussion

### *3.1 UV-Visible Analysis*

The dye component is an important component in the DSSC system. In this study, a combination of sensitized natural dyes was employed, including: (a) sappan wood/E and turmeric/M; (b) turmeric/M and beetroot/E; (c) beetroot/E and turmeric/A, as natural dyes sensitized in the DSSC system. Turmeric, functioning as a natural dye, contains the pigment curcumin.

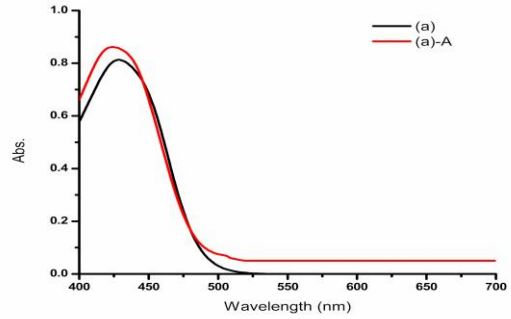


(I)

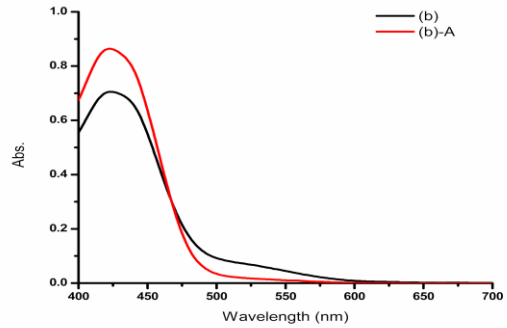


(II)

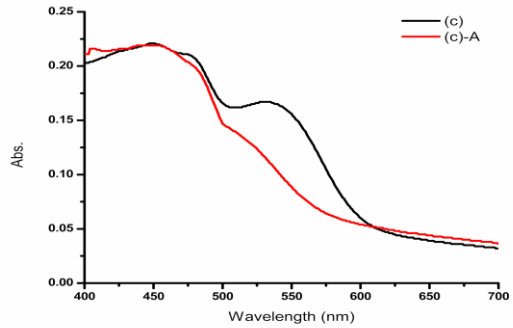


III

**Fig.1** UV-Vis spectrum of (I) sappan wood/E and turmeric/M dyes with normal pH (a) and acidic pH (a)-A; (II) turmeric/M and beetroot/E dyes with normal pH (b) and acidic pH (b)-A; (III) beetroot/E and turmeric/A dyes with normal pH (c) and acidic pH (c)-A

Curcumin is the main compound in turmeric extract and appears as a bright yellow. The absorption spectrum of curcumin extracted from turmeric with methanol is in the range of 350–470 nm, with a strong absorption peak at 427 nm (Kabir *et al.,* 2019). On other hand, sappan wood (*Caesalpinia sappan* L.) as a natural dye source contains homoisoflavonoid, which is responsible for the pigment brazilein, this dye has an absorption wavelength range of 283.4-538.6 nm (Kebede *et al.,* 2022). Fig. 1 (I) shows the highest absorption peaks for the combination of sappan/E and turmeric/M dyes in the wavelength range of 400–550 nm, resulting in peak wavelengths of 422 nm for normal pH (a) and 428 nm for acidic pH (a)-A. The increased cumulative absorption qualities across the region in the UV-Vis absorption spectrum to indicate that the combination of sappan wood and turmeric dyes exhibits superior light absorption in acidic pH conditions, as evidenced by higher absorbance compared to neutral pH settings. While beets contain the pigment betaine, the pigment is soluble in water and alcohol. This dye has an absorption wavelength range of 480–540 nm (Surana *et al.,* 2021; Nouairi *et al.,* 2021). The combination of dyes Fig.1(II) shows the highest absorption peaks for the combination of turmeric/M and beet/E dyes in the wavelength range of 400–700 nm, resulting in peak wavelengths of 422 nm for normal pH (b) and 421 nm for acidic pH (b)-A The increased cumulative absorption qualities across the region in the UV-Vis absorption spectrum to indicate that the combination of sappan wood and turmeric dyes absorbs light better in acidic pH conditions, as evidenced by higher absorbance compared to neutral pH settings. Fig 1(III) shows the highest absorption peaks for the combination of beetroot/E and turmeric/A dyes in the wavelength range of 400–700 nm, giving rise to peaks at 525 nm for normal pH (c) and 450 nm for acidic pH (c)-A The increased cumulative absorption qualities across the region in the UV-Vis absorption spectrum tend to indicate that the combination of sappan wood and turmeric dyes absorbs light better in acidic pH conditions, as evidenced by higher absorbance compared to neutral pH settings. The maximum wavelength absorption pigment of the brazilein/E- curcumin/M (a) dye combination is shown in Fig.1 (I); curcumin/M-betanine/E (b) in Fig. 1 (II); and betanin/M-curcumin/A (c) in Fig. 1 (III). Where the wavelength absorption is the result of mixing the two dyes in the dye combination (a); (b); and (c), situated in the visible light region, which is in the range of 400–750 nm in the dye component of normal and acidic pH conditions.

### *3.2 Voltammetry Cyclic Analysis*

Identification was conducted using voltammetry with analytical data on the blending component using an acidic pH (without pH) conditions, as presented in Table 2. The results report that the natural photosensitizer in the DSSC meets the requirements

**Table 1**
Dye Maximum Wavelength

| | Dye | pH | Wavelength (nm) |
|---|---|---|---|
| (a) | S/E/I & k/M/II | Neutral | 422 |
| | | Acid | 428 |
| (b) | k/M/II & kB/E/I | Neutral | 422 |
| | | Acid | 421 |
| (c) | kB/E/I & k/A/II | Neutral | 525 |
| | | Acid | 450 |

**Table 2**
Voltammetry for component blending dyes

| | Dye | pH | HOMO | LUMO | Bandgap Energy (eV) |
|---|---|---|---|---|---|
| (a) | S/E/I & k/M/II | Normal | -4.29799 | -3.94126 | 0.357 |
| | | Acid | -4.29745 | -3.96278 | 0.335 |
| (b) | k/M/II & kB/E/I | Normal | -4.2977 | -3.91131 | 0.386 |
| | | Acid | -4.29774 | -3.92772 | 0.370 |
| (c) | kB/E/I & k/A/II | Normal | -4.29752 | -4.13384 | 0.164 |
| | | Acid | -4.29751 | -4.00386 | 0.294 |

*S = sappan wood (Biancaea sappan); k = turmeric (Curcuma longa); kB = beetroot (Beta vulgaris); E = Ethanol; M = Methanol; A = Distilled water

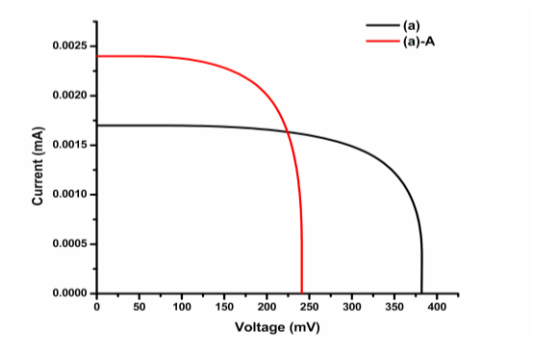


(I)

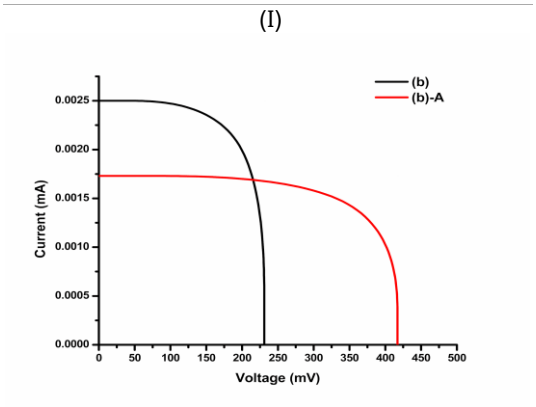


(II)

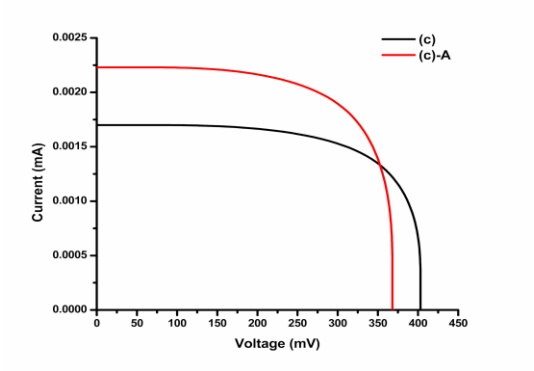


(III)

**Fig.2** I-V Curve (I) sappan wood/E and turmeric/M dyes with normal pH (a) and acidic pH (a)-A; (II) turmeric/M and beetroot dye normal pH (b) and acidic pH (b)-A; (III) beetroot/E and turmeric/A dye normal pH (c) and acidic pH (c)-A.

when the LUMO value of dyes exceeds the LUMO of conduction band of the semiconductor used, specifically $TiO_2$ (-4.0 eV), suggesting that the electron injection from these LUMOs to the $TiO_2$ conduction band is possible (Setiarso et al., 2023). The results indicate that the samples don't significantly differ from one another. However, a reduction in the band gap, especially smallest band gap, can still evident in sample (c) compared to other samples. The short distance between the LUMO and the conduction band of the $TiO_2$ semiconductor shows a significant effect on the band gap results. This is related to the ease with which electrons are released in natural dyes (Hitam & Jalil, 2020; Karthikeyan *et al.,* 2020; Omar *et al.,* 2020; Selvaraj *et al.,* 2021). Conductivity increases as electrons are more easily removed (Mao et al., 2021), thereby impacting the band gap and resulting in a smaller value (Wang *et al.*, 2019).

In a single natural dye, the resulting LUMO is close to the value of the conduction band (Maurya *et al.,* 2019). However, in the case of component mixture dyes, the LUMO is more distant from the band gap (Benson *et al.,* 2020). Sample (a) is larger than a single natural dye and has an impact on reducing the band gap (Pakdel & Peighambardoust, 2018). This happens because the band gap energy is influenced by the length of the lattice parameters in the crystal structure (Ul Islam & Mohd, 2019). The longer the lattice parameter, the smaller the band gap energy (Khan *et al.,* 2020). This is due to the low interatomic bonding force, facilitating easier electron movement (Cao *et al.,* 2021). This significantly influences the distinction between a single dye and blending, resulting in a tendency for a larger band gap energy due to lattice and crystal changes (Nair *et al.,* 2020). In PVDF membranes, a favorable driving force occurs when electrons are injected into the semiconductor surface with a low band gap (Janjua *et al.,* 2021; Daoud *et al.*, 2022; Kusumawati *et al.,* 2023). Hence, the electron regeneration process in dye can occur more rapidly in DSSCs. This means that the membrane will greatly affect the results of the current generated due to samples with a low band gap (Li *et al.,* 2019). As mentioned earlier, a low band gap leads to a high conductivity value due to the easier process of attracting electrons in the dye from the valence band to the conduction band, thus the higher the quality of the dyes. (Bittau *et al.*, 2018). Therefore, the improvement is notably enhanced with the assistance of membranes (Qi *et al.*, 2020).

### *3.3 Photovoltaic Studies*

The short-circuit current (Isc) and open-circuit voltage (Voc) were measured experimentally. The IV characteristics curve was employed to determine Pmax and fill factor (FF), and the cell efficiency was calculated using in equation (1). The characteristics of a solar cell are explained through the current versus voltage curve (I-V curve) (Fig.2). According to the I-V curve the photovoltaic performance parameters, such as open-circuit voltage (Voc), short-circuit current density (Isc), fill factor (FF), and power conversion efficiency (**η**) DSSC, which used with variations in composition and pH can be obtained as

**Table 3**
Studi Photovoltaic

| Dye | pH | Isc (mA/cm$^2$) | Voc (mV) | FF (%) | Efficiency (%) |
|---|---|---|---|---|---|
| (a) S/E/I & k/M/II | Neutral | 1.7 x 10$^{-3}$ | 382 | 3.22 | 2.09 |
| | Acid | 2.4 x 10$^{-3}$ | 241 | 4.48 | 2.59 |
| (b) k/M/II & kB/E/I | Neutral | 2.5 x 10$^{-3}$ | 231 | 3.64 | 2.1 |
| | Acid | 1.73 x 10$^{-3}$ | 417 | 3.31 | 2.39 |
| (c) kB/E/I & k/A/II | Neutral | 1.7 x 10$^{-3}$ | 403 | 3.2 | 2.19 |
| | Acid | 2.23 x 10$^{-3}$ | 363 | 3.35 | 2.71 |

summarized in Table 3. Dyes have an important role in increasing the absorption spectrum of sunlight.

Photoconversion efficiency for DSSCs sensitized with red and yellow colouring pigments were 0.416% and 0.921%, respectively (Abdullah *et al.,* 2022). In the combination of dyes (a) sappan wood/E and turmeric/M with neutral pH, the values of Isc, Voc, and FF are 1.7 x 10$^{-3}$ mA/cm$^2$, respectively; 382 mV; 3.22%; and an efficiency was 2.09%. Meanwhile, at acidic pH, the values of Isc, Voc, and FF are 2.4 x 10$^{-3}$ mA/cm$^2$, respectively; 241 mV; 4.48%; and an efficiency was 2.59%. This shows that the combination of these dyes can increase efficiency compared to the individual efficiency of each dye, and the best efficiency is shown under acidic conditions.

DSSCs sensitized with natural yellow from curcumin pigment in turmeric and natural red from betaine in beetroot pigment have photoconversion efficiencies of 0.378% and 0.15%, respectively (Khan *et al.,* 2020). In the combination of dyes (b) turmeric/M and beetroot/E with neutral pH, the values of Isc, Voc, and FF were 2.5 x 10$^{-3}$ mA/cm$^2$, respectively; 231 mV; 3.64%; and an efficiency was 2.10%. On other hand, at acidic pH, the values of Isc, Voc, and FF are 1.73 x 10$^{-3}$ mA/cm$^2$, respectively; 417 mV; 3.31%; and efficiency was 2.39%. This shows that the combination of these dyes can increase efficiency compared to the individual efficiency of each dye, and the best efficiency is shown under acidic conditions.

In the combination of dyes (c) beetroot/E and turmeric/A with neutral pH, the values of Isc, Voc, and FF were 1.7 x 10$^{-3}$ mA/cm$^2$, respectively; 403 mV; 3.20%; and efficiency was 2.19%. Simultaneously, at acidic pH, the values of Isc, Voc, and FF were 2.23 x 10$^{-3}$ mA/cm$^2$, respectively; 363 mV; 3.35%; and an efficiency was 2.71%. This shows that the combination of these dyes can enhance efficiency compared to the individual efficiency of each dye, with the optimal efficiency observed under acidic conditions.

The efficiency values in the combination of coded dyes (a), (b), and (c) variations at acidic pH variations were higher than those at normal pH variations. The table 3 shows that among the three combinations of natural dyes mentioned above, the highest efficiency is observed in the combination of dyes (c), beetroot/ethanol, and turmeric/distilled water at acidic pH with an efficiency of 2.71%.

## 4. Conclusion

The efficiency values in the combination of coded dyes (a), (b), and (c) at neutral pH variation are 2.09%, 2.10%, and 2.19%, respectively. Meanwhile, the efficiency values are 2.59%, 2.39%, and 2.71% at acidic pH. The combination of dyes at acidic pH conditions demonstrated higher efficiency values compared to the neutral pH variation. Among the three dye combinations, the highest efficiency was observed in the combination of (c) beetroot/ethanol and turmeric/distilled water, reaching 2.71%.

## Acknowledgments

The authors would like to thank the Ministry of Education, Culture, Research, and Technology of the Republic of Indonesia for financial support.

**Author Contributions:** I.W.E.: conceptualization, methodology, investigation, resources, data curation, writing—original draft,review and editing; N.K.: supervision, project administration, writing—review, validation, writing—review and editing; P.S.: formal analysis, writing—review and editing; S.M.: writing—review and editing, formal analysis and data curation; N.T.R.: writing draft, visualization, software, project administration; R.N.S.: investigation, resources, writing, review and editing and validation; N.Z.; writing, review and editing, validation; F.F.F.: investigation, resources, writing and validation. All authors have read and agreed to the published version of the manuscript.

**Funding:** This research was funded by the Ministry of Education, Culture, Research, and Technology of Indonesia Republic, Contract Number B/29559/UN38.9/LK.04.00/2022

**Conflicts of Interest:** The authors declare no conflict of interest.

## References

Abdullah, M. ., Syarifah Adilah, M. ., Noorsal, E., Azurahanim, C. A. ., Mamat, M. ., Ahmad, M. ., I.B.S. Banu, I. B. ., & Rusop, M. (2022). Synergistic effect of complementary organic dye co-sensitizers for potential panchromatic light-harvesting of dye-sensitized solar cells. Optical Materials, 133, 113016. https://doi.org/doi:10.1016/j.optmat.2022.113016

Alirahmi, S. M., Rahmani Dabbagh, S., Ahmadi, P., & Wongwises, S. (2020). Multi-objective design optimization of a multi-generation energy system based on geothermal and solar energy. *Energy Conversion and Management*, *205*(October 2019), 112426. https://doi.org/10.1016/j.enconman.2019.112426

Bandara, T. M. W. J., Weerasinghe, A. M. J. S., Dissanayake, M. A. K. L., Senadeera, G. K. R., Furlani, M., Albinsson, I., & Mellander, B. E. (2018). Characterization of poly (vinylidene fluoride-co-hexafluoropropylene) (PVdF-HFP) nanofiber membrane based quasi solid electrolytes and their application in a dye sensitized solar cell. *Electrochimica Acta*, *266*, 276–283. https://doi.org/10.1016/j.electacta.2018.02.025

Benson, C. R., Kacenauskaite, L., VanDenburgh, K. L., Zhao, W., Qiao, B., Sadhukhan, T., Pink, M., Chen, J., Borgi, S., Chen, C. H.,

Davis, B. J., Simon, Y. C., Raghavachari, K., Laursen, B. W., & Flood, A. H. (2020). Plug-and-Play Optical Materials from Fluorescent Dyes and Macrocycles. *Chem*, *6*(8), 1978–1997. https://doi.org/10.1016/j.chempr.2020.06.029

Bittau, F., Potamialis, C., Togay, M., Abbas, A., Isherwood, P. J. M., Bowers, J. W., & Walls, J. M. (2018). Analysis and optimisation of the glass/TCO/MZO stack for thin film CdTe solar cells. *Solar Energy Materials and Solar Cells*, *187*(July), 15–22. https://doi.org/10.1016/j.solmat.2018.07.019

Bußmann, A. B., Grünerbel, L. M., Durasiewicz, C. P., Thalhofer, T. A., Wille, A., & Richter, M. (2021). Microdosing for drug delivery application—A review. *Sensors and Actuators, A: Physical*, *330*. https://doi.org/10.1016/j.sna.2021.112820

Cao, H., Tang, X., Tang, H., Yuan, Y., & Wu, J. (2021). Photoinduced intermolecular hydrogen atom transfer reactions in organic synthesis. *Chem Catalysis*, *1*(3), 523–598. https://doi.org/10.1016/j.checat.2021.04.008

Daoud, A., Cheknane, A., Meftah, A., Nunzi, J. M., Shalabi, M., & Hilal, H. S. (2022). Spatial separation strategies to control charge recombination and dye regeneration in p-type dye sensitized solar cells. *Solar Energy*, *236*, 107–152. https://doi.org/https://doi.org/10.1016/j.solener.2022.02.050

Ganiyu, S. O., Martínez-Huitle, C. A., & Rodrigo, M. A. (2020). Renewable energies driven electrochemical wastewater/soil decontamination technologies: A critical review of fundamental concepts and applications. *Applied Catalysis B: Environmental*, *270*. https://doi.org/10.1016/j.apcatb.2020.118857

Ganta, D., Combrink, K., & Villanueva, R. (2019). Natural dye-sensitized solar cells: Fabrication, characterization, and challenges. In *Energy, Environment, and Sustainability* (pp. 129–155). Singapore: Springer Singapore. https://doi.org/10.1007/978-981-13-3302-6_5

Golshan, M., Osfouri, S., Azin, R., Jalali, T., & Moheimani, N. R. (2021). Co-sensitization of natural and low-cost dyes for efficient panchromatic light-harvesting using dye-sensitized solar cells. *Journal of Photochemistry and Photobiology A: Chemistry*, *417*(April), 113345. https://doi.org/10.1016/j.jphotochem.2021.113345

Hdom, H. A. D., & Fuinhas, J. A. (2020). Energy production and trade openness: Assessing economic growth, $CO_2$ emissions and the applicability of the cointegration analysis. *Energy Strategy Reviews*, *30*. https://doi.org/10.1016/j.esr.2020.100488

Hitam, C. N. C., & Jalil, A. A. (2020). A review on exploration of Fe2O3 photocatalyst towards degradation of dyes and organic contaminants. *Journal of Environmental Management*, *258*(January), 110050. https://doi.org/10.1016/j.jenvman.2019.110050

Jalali, T., Arkian, P., Golshan, M., Jalali, M., & Osfouri, S. (2020). Performance evaluation of natural native dyes as photosensitizer in dye-sensitized solar cells. *Optical Materials*, *110*(110441), 110441. https://doi:10.1016/j.optmat.2020.110441

Janjua, M. R. S. A., Khan, M. U., Khalid, M., Ullah, N., Kalgaonkar, R., Alnoaimi, K., Baqader, N., & Jamil, S. (2021). Theoretical and Conceptual Framework to Design Efficient Dye-Sensitized Solar Cells (DSSCs): Molecular Engineering by DFT Method. *Journal of Cluster Science*, *32*(2), 243–253. https://doi.org/10.1007/s10876-020-01783-x

Ji, L., Yuxuan, W., Sun, L., Xiaohu, Z., Wang, X., Xie, Y., Guo, J., & Huang, G. (2022). Solar photovoltaics can help China fulfill a net-zero electricity system by 2050 even facing climate change risks. *Resources, Conservation and Recycling*, *186*, 106596. https://doi.org/https://doi.org/10.1016/j.resconrec.2022.106596

Junger, Udomrungkhajornchai, Grimmelsmann, Blachowicz, & Ehrmann. (2019). Effect of caffeine copigmentation of anthocyanin dyes on DSSC efficiency. *Materials*, *12*(17), 2692. https://doi:10.3390/ma12172692

Kabir, F., Bhuiyan, M. M. H., Manir, M. S., Rahaman, M. S., Khan, M. A., & Ikegami, T. (2019). Development of dye-sensitized solar cell based on combination of natural dyes extracted from Malabar spinach and red spinach. *Results in Physics*, *14*(June), 102474. https://doi.org/10.1016/j.rinp.2019.102474

Karthikeyan, C., Arunachalam, P., Ramachandran, K., Al-Mayouf, A. M., & Karuppuchamy, S. (2020). Recent advances in semiconductor metal oxides with enhanced methods for solar photocatalytic applications. *Journal of Alloys and Compounds*, *828*, 154281. https://doi.org/10.1016/j.jallcom.2020.154281

Kebede, A. A., Kalogiannis, T., Van Mierlo, J., & Berecibar, M. (2022). A comprehensive review of stationary energy storage devices for large scale renewable energy sources grid integration. *Renewable and Sustainable Energy Reviews*, *159*, 112213. https://doi.org/10.1016/j.rser.2022.112213

Khan, M. I., Arshad, H., Rizwan, M., Gillani, S. S. A., Zafar, M., Ahmed, S., & Shakil, M. (2020). Investigation of structural, electronic, magnetic and mechanical properties of a new series of equiatomic quaternary Heusler alloys CoYCrZ (Z = Si, Ge, Ga, Al): A DFT study. *Journal of Alloys and Compounds*, *819*, 152964. https://doi.org/10.1016/j.jallcom.2019.152964

Kusumawati, N., Setiarso, P., & Muslim, S. (2018). Polysulfone/polyvinylidene fluoride composite membrane: Effect of coating dope composition on membrane characteristics and performance. *Rasayan Journal of Chemistry*, *11*(3), 1034–1041. https://doi.org/10.31788/RJC.2018.1133020

Kusumawati, N., Setiarso, P., Muslim, S., & Purwidiani, N. (2018). Synergistic ability of PSf and pvdf to develop high-performance PSf/PVDF coated membrane for water treatment. *Rasayan Journal of Chemistry*, *11*(1), 260–279. https://doi.org/10.7324/RJC.2018.1112018

Kusumawati, Nita, Setiarso, P., Santoso, A. B., Muslim, S., A'yun, Q., & Putri, M. M. (2023). Characterization of Poly(vinylidene Fluoride) Nanofiber-Based Electrolyte and Its Application to Dye-Sensitized Solar Cell with Natural Dyes. *Indonesian Journal of Chemistry*, *23*(1), 113–126. https://doi.org/10.22146/ijc.75357

Kusumawati, Nita, Setiarso, P., Sianita, M. M., & Muslim, S. (2018). Transport properties, mechanical behavior, thermal and chemical resistance of asymmetric flat sheet membrane prepared from PSf/PVDF blended membrane on gauze supporting layer. *Indonesian Journal of Chemistry*, *18*(2), 257–264. https://doi.org/10.22146/ijc.27272

Li, B., Meng, M., Cui, Y., Wu, Y., Zhang, Y., Dong, H., Zhu, Z., Feng, Y., & Wu, C. (2019). Changing conventional blending photocatalytic membranes (BPMs): Focus on improving photocatalytic performance of $Fe_3O_4$/g-$C_3N_4$/PVDF membranes through magnetically induced freezing casting method. *Chemical Engineering Journal*, *365*(November 2018), 405–414. https://doi.org/10.1016/j.cej.2019.02.042

Mao, W., Zhang, L., Liu, Y., Wang, T., Bai, Y., & Guan, Y. (2021). Facile assembled N, S-codoped corn straw biochar loaded Bi2WO6 with the enhanced electron-rich feature for the efficient photocatalytic removal of ciprofloxacin and Cr(VI). *Chemosphere*, *263*, 127988. https://doi.org/10.1016/j.chemosphere.2020.127988

Maurya, I. C., Singh, S., Srivastava, P., Maiti, B., & Bahadur, L. (2019). Natural dye extract from Cassia fistula and its application in dye-sensitized solar cell: Experimental and density functional theory studies. *Optical Materials*, *90*(October 2018), 273–280. https://doi.org/10.1016/j.optmat.2019.02.037

Mejica, G. F. C., Unpaprom, Y., Balakrishnan, D., Dussadee, N., Buochareon, S., & Ramaraj, R. (2022). Anthocyanin pigment-based dye-sensitized solar cells with improved pH-dependent photovoltaic properties. *Sustainable Energy Technologies and Assessments*, *51*(101971), 101971. https://doi.org/10.1016/j.seta.2022.101971

Moharam, M. M., El Shazly, A. N., Anand, K. V., Rayan, D. E. R. A., Mohammed, M. K. A., Rashad, M. M., & Shalan, A. E. (2021). Semiconductors as Effective Electrodes for Dye Sensitized Solar Cell Applications. *Topics in Current Chemistry*, *379*(3), 1–17. https://doi.org/10.1007/s41061-021-00334-w

Morsada, Z., Hossain, M. M., Islam, M. T., Mobin, M. A., & Saha, S. (2021). Recent progress in biodegradable and bioresorbable materials: From passive implants to active electronics. *Applied Materialstoday*, *25*, 101257. https://doi.org/https://doi.org/10.1016/j.apmt.2021.101257

Nair, G. B., Swart, H. ., & Dhoble, S. . (2020). A review on the advancements in phosphor-converted light emitting diodes (pc-LEDs): Phosphor synthesis, device fabrication and characterization. *Progress in Materials Science*, *109*, 100622. https://doi.org/https://doi.org/10.1016/j.pmatsci.2019.100622

Noorasid, N. S., F, A., Mustafa, A. ., Azam, M. ., Mahalingam, S Chelvanathan, P., & Amin, N. (2022). Current advancement of flexible dye sensitized solar cell: A review. *Optics*, *254*, 168089. https://doi.org/https://doi.org/10.1016/j.ijleo.2021.168089

Nouairi, M. E. A., Freha, M., & Bellil, A. (2021). Study by absorption and emission spectrophotometry of the efficiency of the binary mixture (Ethanol-Water) on the extraction of betanin from red beetroot. *Spectrochimica Acta - Part A: Molecular and Biomolecular Spectroscopy*, *260*, 119939. https://doi.org/10.1016/j.saa.2021.119939

Omar, A., Ali, M. S., & Abd Rahim, N. (2020). Electron transport properties analysis of titanium dioxide dye-sensitized solar cells ($TiO_2$-DSSCs) based natural dyes using electrochemical impedance spectroscopy concept: A review. *Solar Energy*, *207*(June 2021), 1088–1121. https://doi.org/10.1016/j.solener.2020.07.028

Önen, T., Karakuş, M. Ö., Coşkun, R., & Çetin, H. (2019). Reaching stability at DSSCs with new type gel electrolytes. *Journal of Photochemistry and Photobiology A: Chemistry*, *385*. https://doi.org/10.1016/j.jphotochem.2019.112082

Pakdel, P. M., & Peighambardoust, S. J. (2018). Review on recent progress in chitosan-based hydrogels for wastewater treatment application. *Carbohydrate Polymers*, *201*, 264–279. https://doi.org/10.1016/j.carbpol.2018.08.070

Panagopoulos, A. (2021). Water-energy nexus: desalination technologies and renewable energy sources. *Environmental Science and Pollution Research*, *28*(17), 21009–21022. https://doi.org/10.1007/s11356-021-13332-8

Pradhan, S. K., & Chakraborty, B. (2020). Substrate materials and novel designs for bipolar lead-acid batteries: A review. *Journal of Energy Storage*, *32*(April), 101764. https://doi.org/10.1016/j.est.2020.101764

Qi, K., Xing, X., Zada, A., Li, M., Wang, Q., Liu, S. yuan, Lin, H., & Wang, G. (2020). Transition metal doped ZnO nanoparticles with enhanced photocatalytic and antibacterial performances: Experimental and DFT studies. *Ceramics International*, *46*(2), 1494–1502. https://doi.org/10.1016/j.ceramint.2019.09.116

Rajaraman, T. S., Gandhi, V. G., Nguyen, V. H., & Parikh, S. P. (2022). Aluminium foil-assisted $NaBH_4$ reduced $TiO_2$ with surface defects for photocatalytic degradation of toxic fuchsin basic dye. *Applied Nanoscience (Switzerland)*, *13*(6), 3925–3944. https://doi.org/10.1007/s13204-022-02628-x

Rekha, M., Kowsalya, M., Ananth, S., Vivek, P., & Jauhar, R. O. M. U. (2019). Current–voltage characteristics of new organic natural dye extracted from Terminalia chebula for dye-sensitized solar cell applications. *Journal of Optics*, *48*(1), 104–112. https://doi:10.1007/s12596-018-0507-5

Setiarso, P., Harsono, R. V., & Kusumawati, N. (2023). Fabrication of Dye Sensitized Solar Cell (DSSC) Using Combination of Dyes Extracted from Curcuma (Curcuma xanthorrhiza) Rhizome and Binahong (Anredera cordifolia) Leaf with Treatment in pH of the Extraction. Indonesian Journal of Chemistry, 23(4), 924–936. https://doi.org/10.22146/ijc.77860

Sharma, K., Sharma, V., & Sharma, S. S. (2018). Dye-sensitized solar cells: Fundamentals and current status. *Nanoscale Research Letters*, *13*(1). https://doi:10.1186/s11671-018-2760-6

Selvanathan, V., Yahya, R., Alharbi, H. F., Alharthi, N. H., Alharthi, Y. S., Ruslan, M. H., Amin, N., & Akhtaruzzaman, M. (2020). Organosoluble starch derivative as quasi-solid electrolytes in DSSC: Unravelling the synergy between electrolyte rheology and photovoltaic properties. *Solar Energy*, *197*(August 2019), 144–153. https://doi.org/10.1016/j.solener.2019.12.074

Selvaraj, V., Swarna Karthika, T., Mansiya, C., & Alagar, M. (2021). An over review on recently developed techniques, mechanisms and intermediate involved in the advanced azo dye degradation for industrial applications. *Journal of Molecular Structure*, *1224*. https://doi.org/10.1016/j.molstruc.2020.129195

Sunder Sharma, S., Sharma, K., Singh, R., Srivastava, S., Bihari Rana, K., & Singhal, R. (2021). Natural pigments: Origin and applications in dye sensitized solar cells. *Materials Today: Proceedings,* 42, 1744–1748. https://doi:10.1016/j.matpr.2020.10.979

Surana, K., Bhattacharya, B., & Majumder, S. (2021). Extraction of yellow fluorescent Caesalpinia sappan L. dye for photovoltaic application. *Optical Materials*, *119*(March), 111347. https://doi.org/10.1016/j.optmat.2021.111347

Ul Islam, S. A., & Mohd, I. (2019). Structural stability improvement, Williamson Hall analysis and band-gap tailoring through A-site Sr doping in rare earth based double perovskite La2NiMnO6. *Rare Metals*, *38*(9), 805–813. https://doi.org/10.1007/s12598-019-01207-4

Wang, S., Zhao, M., Zhou, M., Li, Y. C., Wang, J., Gao, B., Sato, S., Feng, K., Yin, W., Igalavithana, A. D., Oleszczuk, P., Wang, X., & Ok, Y. S. (2019). Biochar-supported nZVI (nZVI/BC) for contaminant removal from soil and water: A critical review. *Journal of Hazardous Materials*, *373*, 820–834. https://doi.org/10.1016/j.jhazmat.2019.03.080

Wu, X., Li, C., Shao, L., Meng, J., Zhang, L., & Chen, G. (2021). Is solar power renewable and carbon-neutral: Evidence from a pilot solar tower plant in China under a systems view. *Renewable and Sustainable Energy Reviews*, *138*(December 2020), 110655. https://doi.org/10.1016/j.rser.2020.110655